NEOPLASIA
www.neoplasia.com

Volume 11 Number 7 July 2009 pp. 662–671 662

Defective Infiltration of Natural Killer Cells in MICA/B–Positive Renal Cell Carcinoma Involves β_2-Integrin–Mediated Interaction[1]

Giuseppe Sconocchia*,†,2, Giulio Cesare Spagnoli†,2, Domenico Del Principe‡, Soldano Ferrone§, Maurizio Anselmi†,‡, Wachanan Wongsena¶, Valerio Cervelli#, Elke Schultz-Thater†, Stephen Wyler†, Vincenza Carafa, Holger Moch††, Luigi Terracciano** and Luigi Tornillo****

*CNR, Institute for Organ Transplantation and Immunocytology, Rome, Italy; †Institute for Surgical Research and Hospital Management, University of Basel, Basel, Switzerland; ‡Department of Pediatrics, University of Rome, Tor Vergata, Rome, Italy; §University of Pittsburgh Cancer Institute, Departments of Surgery, Immunology and Pathology, Pittsburgh, PA, USA; ¶Department of Medical Technology, Faculty of Allied Health Sciences, Naresuan University, Phitsanulok, Thailand; #Department of Surgery, University of Rome "Tor Vergata," Rome, Italy; **Institute of Pathology, University of Basel, Basel, Switzerland; ††Institute of Pathology, University of Zurich, Zurich, Switzerland

Abstract

We have explored MICA/B expression and its relationship with innate inflammatory infiltrate in renal cell carcinoma (RCC). The expression of MICA/B, CD16, CD56, and CD68 in 140 RCC lesions contained in a tissue microarray (TMA) was investigated by immunohistochemistry. MICA/B gene and protein expressions in Caki-1 cells were analyzed by reverse transcription–polymerase chain reaction and flow cytometry, respectively. Natural killer (NK) cells were studied by flow cytometry. All the RCC lesions ($n = 140$) were MICA/B–positive. MICA/B was mainly expressed in the cytoplasm of tumor cells, whereas stromal cells were negative. Renal cell carcinoma lesions showed low NK cell infiltration, although they were rich in $CD16^+CD56^-$ cells, strongly resembling macrophages. $CD16^+$ macrophage infiltration was more frequently detectable in metastatic lesions compared with primary tumors ($P = .0223$) and was associated with poor RCC differentiation ($P = .007$). To investigate mechanisms potentially underlying the lack of NK cells infiltration into MICA/B–positive RCC lesions, we used Caki-1 RCC cells. Caki-1 expressed *MICA* and *MICB* genes. However, MICA protein was not detectable in Caki-1 cells, whereas MICB protein was detectable in their cytoplasm and on the cell membrane. Coculture of peripheral blood mononuclear cells with Caki-1, K562, HCT116, respectively, resulted in $CD56^+CD16^+$ NK cells deletion without affecting $CD56^+/CD16^-$ NK subset and immature NK cells generated *in vitro* from $CD34^+$ cells. Natural killer cell apoptosis seemed to be preferentially triggered by cancer cells because HLA-A0201$^+$ NK cells were only marginally affected by allogeneic HLA-A0201$^-$ peripheral blood mononuclear cells. Caki-1 cell–mediated NK cell apoptosis was reduced by an anti–β_2-integrin (CD18) monoclonal antibody but was NKG2D-, granule exocytosis–, and caspase-independent.

Neoplasia (2009) 11, 662–671

Address all correspondence to: Dr. Giuseppe Sconocchia, Institute for Surgical Research and Hospital, Management, University of Basel, ZLF Hebelstrasse 20, 4031 Basel, Switzerland. E-mail: giuseppe.sconocchia@cnr.it, sconocchiag@yahoo.com

[1]This work has been supported by The Italian National Council Research (CNR, funding, ME.P03.009), Swiss National Fund for Scientific Research (grant to G.C.S.), Rainbow Onlus Association for Research in Pediatric Oncology-Hematology, Rome, Italy.
[2]These authors have equally contributed to this study.
Received 9 February 2009; Revised 9 April 2009; Accepted 9 April 2009

DOI 10.1593/neo.09296

Introduction

Advanced renal cell carcinoma (RCC) is a fatal disease with a median survival of approximately 1 year [1,2]. Nevertheless, RCC is considered to be a malignancy potentially susceptible to innate and adaptive immune responses of the host because a small subset of patients with advanced disease achieves spontaneous or immunotherapy-induced complete remission [3–5]. The cellular and molecular mechanisms underlying these complete remissions are not completely understood, although a variety of inflammatory cells including T and Natural killer (NK) cells have been identified in RCC lesions [6].

Approximately 90% of RCC lesions express HLA-class I antigens [7]. According to the missing self hypothesis [8,9], the immunological control of RCC is likely to be ascribed to T cells rather than to NK cells because NK cell's cytotoxicity is negatively regulated by HLA-class I expression on malignant cells through its interaction with killer inhibitory receptors (KIRs) [10]. However, recent findings have underlined that *de novo* expression of NKG2D ligands (NKG2DLs) on HLA-class I antigen–positive malignant cells restores sensitivity to NK cell–mediated cytotoxicity despite HLA matching [11], thus reevaluating the potential role of NK cells in controlling HLA-class I–positive malignancies [12].

Nonclassic HLA-class I antigen–related molecules MICA and MICB are major ligands of NKG2D and are often expressed on cancer cells. They share 84.3% of amino acids sequence identity and are highly polymorphic.

The expression of NKG2DLs, MICA/B, and its relationship with infiltration of the tumor microenvironment by inflammatory cells in RCC specimens have not clearly been investigated so far. Using a home-made monoclonal antibody (mAb) recognizing a common epitope of MICA and MICB (MICA/B–specific), WW6B7, we stained a tissue microarray (TMA) composed of 140 RCC lesions: we present evidence that cultured renal cancer cells and clinical RCC specimens express MICA/B. Most interestingly, however, these tumors are characterized by inflammatory infiltrates poor in NK cells and enriched in $CD16^+$ macrophages. Infiltration of RCC lesions by these cells may have clinical significance because it is associated with advanced stage of the disease and poor grade of differentiation. Data from *in vitro* model developed to address underlying mechanisms suggest that these finding may reflect NK cell deletion by RCC cells due to apoptosis involving β_2-integrin, CD18–mediated interaction.

Materials and Methods

Cell Lines

The RCC cell line Caki-1, the NK cell–sensitive myeloid cell line K562, the cervical carcinoma cell line HeLa, the melanoma cell line D10, and the colorectal carcinoma (CRC) cell line HCT116 were cultured in OptiMem reduced serum medium (Invitrogen, Carlsbad, CA) supplemented with 5% FBS.

Antibodies and Reagents

The generation and the specificity of the MICA/B mAb, WW2G8, have been described elsewhere [11]. The MICA/B mAb WW6B7 was generated in our laboratory using the methodology of Kohler and Milstein [13]. The specificity of mAb WW6B7 was determined by Western blot and flow cytometry analysis of $MICA^+$ and $MICA^-$ cell lines and $MICB^+$ and $MICB^-$ transfectants. Allophycocyanin (APC)-conjugated anti-MICB, phycoerythrin (PE)-conjugated anti-MICA and anti-NKG2D mAbs were purchased from R&D Systems (Abingdon, United Kingdom). Biotinylated anti-CD16, biotinylated anti-CD56, and matching isotype mouse mAbs were purchased from DAKO (Glostrup, Denmark) and Novocastra (Newcastle, United Kingdom). Fluorescein isothiocyanate (FITC)–conjugated anti-FcγIII (anti-CD16), PE-conjugated anti-CD56, peridinin chlorophyl protein–conjugated anti-CD56, APC-conjugated anti-CD3 mAbs, FITC-conjugated goat–anti–mouse immunoglobulin G (IgG) $F(ab)_2$ antibodies, and annexin V–FITC apoptosis detection kit I were purchased from BD Bioscience (San Jose, CA). Magnetic bead–conjugated anti-CD34 and anti-CD56 mAbs were purchased from Miltenyi Biotec (Miltenyi Biotech, Bergisch Gladbach, Germany). Purified anti-CD18 was purchased from BD Bioscience. Interleukin 2 (IL-2) and stem cell factor (SCF) were purchased from Hoffmann-LaRoche (Basel, Switzerland) and Peprotech (Rocky Hill, NJ), respectively. Concanamycin A was purchased from Sigma Chemical, Co. (St. Louis, MO). The general caspase inhibitor, Z-VAD-FMK, was purchased from BD Bioscience.

Cell Isolation Activation and Expansion

Peripheral blood mononuclear cells (PBMCs) were isolated by Ficoll-Hypaque density gradient separation. Cells were cultured in RPMI 1640 medium supplemented with 10% fetal calf serum, glutamine (2 mM), and gentamicin, thereafter referred to as complete medium (CM).

Healthy stem cell donors gave permission for a fraction of their $CD34^+$ cells to be used for research under institutional review board–approved National Hearth Lung and Blood Institute (National Institutes of Health, Bethesda, MD) stem cell allotransplantation protocols. $CD34^+$ cells were isolated as previously described [11,14], counted, and frozen in liquid nitrogen until use. $CD34^+$ cells were then cultured in CM in 96-well U-bottom plates (Costar, Corning, NY) for 21 days. Cells were stimulated every 5 days with 50 ng/ml SCF and recombinant IL-2 (200 U/ml). To obtain a purified $CD56^+$ cell population, $CD34^+$ cells cultured in SCF and IL-2 or PBMC stimulated for 4 days with IL-2 were stained with magnetic bead–conjugated anti-CD56 mAb (Miltenyi Biotech) and passed through a magnetic column. In the absence of magnet, a vigorous mechanic pressure sufficed to elute $CD56^+$ cells retained in the column.

Reverse Transcription–Polymerase Chain Reaction

Total RNA was extracted from 3×10^6 cultured cells using a Qiagen (Basel, Switzerland) RNeasy kit. Complementary DNA (cDNA) first strand was produced using a SuperScript First-Strand Synthesis System using $oligo(dt)^{12\text{-}18}$ antisense primers (Invitrogen, Lucerne, Switzerland). *MICA* and *MICB* transcripts were amplified from cDNA by 30 cycles of polymerase chain reaction in the presence of the following primers: *MICA*/*MICB* sense primer (5′ACACCCAGCAGTGGGGGGAT3′); *MICA* antisense primer (5′GCAGGGAATTGAATCCCAGCT3′); and *MICB* antisense primer (5′AGCAGTCGTGAGTTTGCCCAC-3′) [15]. The amplification conditions consisted of denaturizing (95°C for 60 seconds), followed by annealing (56°C for 60 seconds), and extension (72°C for 60 seconds). Amplified fragments were analyzed in 1.5% agarose gel electrophoresis in the presence of ethidium bromide (Sigma).

Flow Cytometry

Magnetically sorted $CD56^+$ cells were cultured in CM in the presence of Caki-1 cells for 8 to 12 hours at 37°C in a 5% CO_2 atmosphere. Nonadherent cells were harvested and stained with a PE-conjugated

anti-CD56 and with an APC-conjugated anti-CD3 mAbs for 30 minutes at 4°C. Cells were washed twice in PBS and stained for 15 minutes in the dark at room temperature in the presence of FITC–annexin V and propidium iodide diluted in 0.5 ml of an appropriate buffer. On the basis of a profound difference between NK cell and Caki-1 cell size scatter, cells were analyzed after three- to four-color staining by defining an electronic gate on lymphocytes area using a FACSCalibur flow cytometer (Becton-Dickinson). For the analysis of the impact of PBMC on allogeneic NK cells, HLA-A0201$^-$ and HLA-A0201$^+$ PBMC from healthy donors were cultured in the presence of IL-2 for 5 days. Cells were then mixed and cultured for 8 to 12 hours, harvested and stained with an APC-conjugated anti-HLA-A0201 mAb, and PE-conjugated anti-CD56 mAb and a PE-Cy5–conjugated anti-CD16 mAb. Cells were washed and stained with FITC-conjugated annexin V as above indicated. Natural killer cells apoptosis was detected by posting an electronic gate on HLA-A0201$^+$ CD16$^+$ cells. To exclude CD16$^+$ small monocytes, we analyzed only CD56$^+$annexin V$^+$ cells.

Relative apoptosis units (RAUs) were calculated giving 100 apoptosis units to the annexin V + NK cell value obtained in the presence of cancer cells at PBMC/cancer cell ratio of 4:1. Then, RAUs were calculated as follows: RAU = % of annexin V + NK cells without cancer cells/% of annexin V + NK cells with cancer cells × 100.

Proliferation Assays

Peripheral blood (PB) CD56$^+$ cells and immature CD56$^+$ cells were magnetically sorted and cultured (1.5×10^5/ml) in the presence of K562 cells at a 2:1 effector/target ratio. After a 3-day culture at 37°C, CD56$^+$ cells were magnetically sorted and counted. Then, 100-μl aliquots of cell cultures depleted of CD56$^+$ cells were transferred in a 96-U/well containing 100 μl of fresh CM and incubated for 2 days at 37°C in a 5% CO_2 atmosphere. Cells were then pulsed with tritiated thymidine (^{3}H-TdR; 1 μCi/well; Amersham Biosciences, Piscataway, NJ). After an additional 18-hour incubation at 37°C, ^{3}H-TdR incorporation was measured using a beta scintillation counter.

RCC Specimens and TMA

TMAs were constructed using formalin-fixed, paraffin-embedded tissue blocks from RCC resections representing part of the tissue specimen collection of the Institute of Pathology, University of Basel (Basel, Switzerland). Representative regions of each tumor were identified using hematoxylin and eosin–stained slides from each block. Tissue cylinders with a diameter of 0.6 mm were punched from the tumor areas of each block (RCC punches) and transferred into a recipient paraffin block using a home-made semiautomated tissue arrayer. MICA/B was detected using mAb WW6B7 and a secondary biotinylated rabbit–anti–mouse IgG antibody. CD16 and CD56 were detected by staining with biotinylated anti-CD16 and anti-CD56 mAbs. One hundred forty RCC lesions were evaluated in this study. To evaluate correlation with tumor grade, 130 RCC lesions were included in the analysis, whereas 10 RCC lesions were excluded because no grading information was available. For tumor stage, we investigated 121 RCC lesions divided as follows: 43 were identified as primary and 78 were identified as metastatic RCC. Nineteen specimens were excluded from the analysis because no information on staging was available.

To evaluate CD16$^+$ cell level of infiltration, the absolute number of infiltrating CD16$^+$ cell was counted in each RCC lesion. For statistical analysis, the level of CD16$^+$ infiltrating cells was considered low when 100 cells or less (score 1) per punch were detected and high when the absolute number of infiltrating CD16$^+$ cells was greater than 100 (score 2).

Statistical Analysis

The significance of statistical differences between the low (score 1) and high levels (score 2) of CD16$^+$ cell infiltration in relationship with tumor grade and stage was assessed by using a χ^2 test. Analysis of NK cell deletion was performed by using Wilcoxon tests and *t* tests.

Results

Expression of MICA/B in RCC Lesions

Incubation with MICA/B–specific mAb WW6B7 of the TMA under investigation, including 140 RCC lesions, resulted in the staining of virtually all (>95%) punches. The staining was generally of strong intensity (Figure 1*A*) and localized in the cytoplasm and cell membranes of cancer cells, whereas it was undetectable in the stromal cells (Figure 1, *B* and *C*) frequently associated with RCC.

Predominance of CD56$^-$/CD16$^+$ Cells in the RCC Inflammatory Infiltrate

We analyzed the nature of the inflammatory cells infiltrating RCC lesions by comparatively evaluating the expression of CD56 and CD16 in the TMA under investigation. Surprisingly, the CD56$^+$/CD16$^+$ cell ratio in the RCC microenvironment was generally lower than 1 (Figure 2*A*), suggesting that a predominant number of CD16$^+$ cells were CD56$^-$. These CD16$^+$CD56$^-$ cells showed a large size and complex morphology, strongly resembling macrophages (Figure 2*B*). Conversely, CD56 expression was predominantly observed on the cell membranes of cancer cells in approximately 25% of the RCC specimens analyzed and was only minimally detectable in RCC infiltrating inflammatory cells (Figure 2*A*, *right*, *lower panel*). Further analysis of RCC microenvironment demonstrated the prevailingly myeloid, CD68$^+$, nature of the inflammatory CD16$^+$ infiltrate (data not shown). To quantify the discrepancy between the expression of CD16 and CD56 inflammatory infiltrate, we compared the absolute number of CD16$^+$ cell infiltration with that of infiltrating CD56$^+$ cells in 108 available RCC lesions. Figure 2*C* clearly shows that most of the CD16$^+$ cells were CD56$^-$, and the level of CD56$^+$ cells into the RCC microenvironment was negligible.

Association of CD16$^+$ Macrophage Infiltration with Cell Differentiation and Disease Progression in RCC

Clinical features associated with RCC infiltration by CD16$^+$ cells were then analyzed. A high level, score 2 (Materials and Methods), of CD16$^+$ cell infiltration was significantly .023 more frequently detectable in metastatic than in primary RCC lesions. As shown in Table 1, a score 2 of CD16$^+$ cell infiltration was only identified in 6 of 43 RCC primary lesions, whereas it was detectable in 25 of 78 metastatic RCC lesions. In contrast, there was no statistically significant difference between score 1 of CD16$^+$ cell infiltration of primary and that of metastatic RCC lesions. Furthermore, high-level, score 2, CD16$^+$ cell infiltration was also significantly ($P = .007$) associated with poor differentiation (G3 and G4) of RCC cells, suggesting that high-grade tumors might shape their microenvironment by recruiting CD16$^+$ myeloid cells.

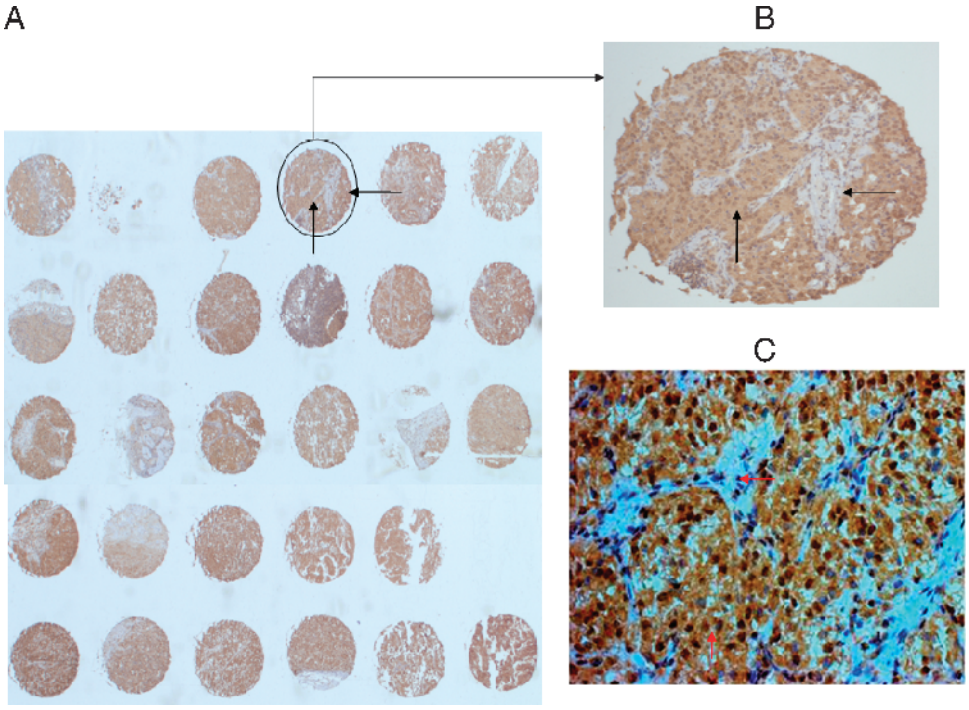

Figure 1. MICA/B expression in RCC TMA. (A) Punches shown in this panel are derived from a randomly selected area of a slide containing 140 RCC lesions stained with WW6B7 mAb. The TMA methodology and WW6B7 mAb staining are described in the Materials and Methods section. Positive cells are stained in brown. (B) An enlargement (×20) of the indicated punches. (C) Detail of an RCC punch containing tumor cells, stroma, and inflammatory infiltrates at an original magnification of ×40. Horizontal arrows indicate interstitial cells, whereas vertical arrows indicate RCC cells.

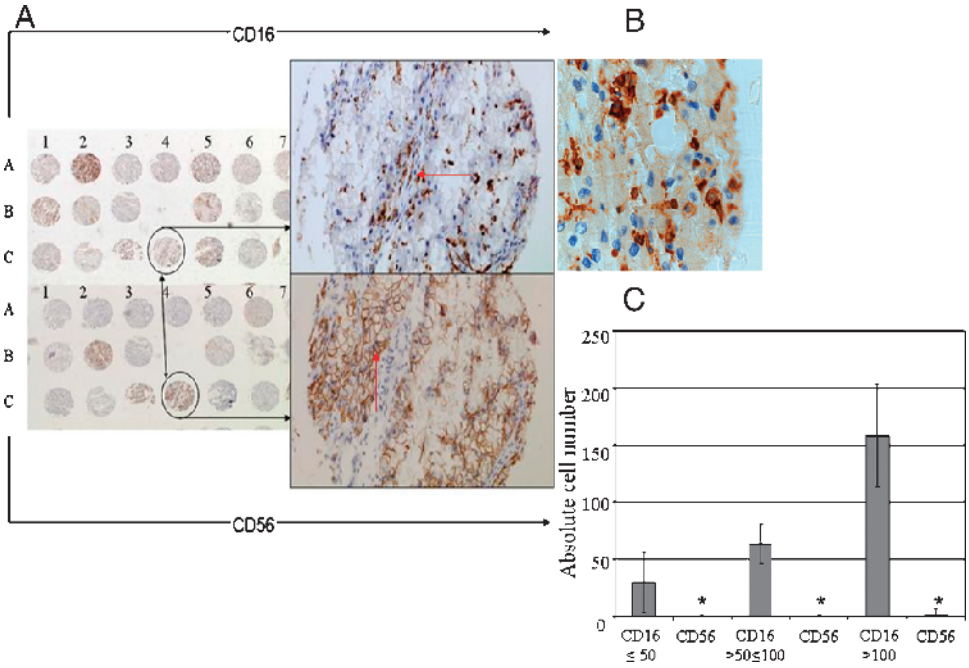

Figure 2. Renal cell carcinoma inflammatory infiltrates is mainly composed of $CD16^+$ macrophages. (A) Two serial sections of RCC lesions (upper and lower panels) taken from the same areas of RCC specimens used for the construction of the indicated TAM. The punches in the upper panel were stained with a biotinylated anti-CD16 mAb, whereas those in the lower panel were stained with a biotinylated anti-CD56 mAb. Upper and lower right panels represent an enlargement of the indicated punches. Panel-positive cells are stained in brown. In either case, original magnifications of ×20 are reported. (B) Detailed morphology of $CD16^+$ cells identified in the indicated RCC area (original magnification, ×60). A, right panel: Horizontal arrow indicates $CD16^+$ interstitial cells, whereas vertical arrow indicates $CD56^+$ RCC cells. (C) Absolute number of low levels of $CD16^+$ cell infiltrate (≤50) and their relative $CD56^+$ infiltrate, $n = 48$; intermediate levels of $CD16^+$ cell infiltration and their relative $CD56^+$ cell infiltration, $n = 32$; and high levels of $CD16^+$ cell infiltration and their relative $CD56^+$ cell infiltration, $n = 28$. Asterisks indicate $CD56^+$ cell infiltrate.

Table 1. Association of the Level of CD16$^+$ Cell Infiltration with Disease Progression and Cancer Cell Differentiation in RCC.

CD16$^+$ Cells	Score 1	Score 2	*P*
RCC stage			
Primary RCC	37 (86%)	6 (14.0%)	
Metastatic RCC	53 (68%)	25 (32.0%)	.023*
RCC grade			
G1 + G2	35 (87.5%)	5 (12.5%)	
G3 + G4	59 (65.5%)	31 (34.4%)	.0070*

G indicates RCC grade of differentiation.
*Statistically significant *P* value.

Expression and Distribution of MICA and MICB by Human RCC Cell Line, Caki-1

The defective NK cell infiltration in RCC lesions with high MICA/B NKG2DL expression prompted us to investigate the underlying mechanism(s) using an *in vitro* model.

First, we analyzed MICA and MICB gene and protein expressions in the RCC cell line, Caki-1, by reverse transcription–polymerase chain reaction and flow cytometry analysis. Caki-1 cells clearly express *MICA* and *MICB* genes (Figure 3*A*). Interestingly, however, surface expression of MICB protein on Caki-1 cells was relatively low, whereas MICA was undetectable. In contrast, HeLa cells were MICA highly positive but MICB-negative, whereas K562 were MICA-negative but MICB-positive (Figure 3*B*).

To investigate the intracellular NKG2DL expression, permeabilized Caki-1 cells were incubated with anti-MICA–specific mAb WW2G8 or with anti-MICA/B mAb WW6B7. As shown in Figure 3*C*, mAb WW2G8 did not stain Caki-1 cells but stained HeLa cells, indicating that MICA was neither on the surface nor intracellular. MICA/B–specific WW6B7 mAb stained Caki-1, D10, and HeLa cells. Most interesting, the staining intensity of permeabilized Caki-1 cells was higher than that of nonpermeabilized cells (Figure 3*D*). In contrast, the staining patterns of nonpermeabilized and permeabilized HeLa cells were similar. These results suggest that the MICB molecule is partially retained in Caki-1 cell cytoplasm and partially transported to cell surface. These results matched immunohistochemistry data showing NKG2DL expressed in the cytoplasm and on the cell surface of RCC cells.

CD56$^+$ Cell and Caki-1 Cell Interaction Results in Mutual Deletion

To investigate whether the defective NK cell infiltration in RCC lesions reflected a deletion of NK cells upon interaction with RCC

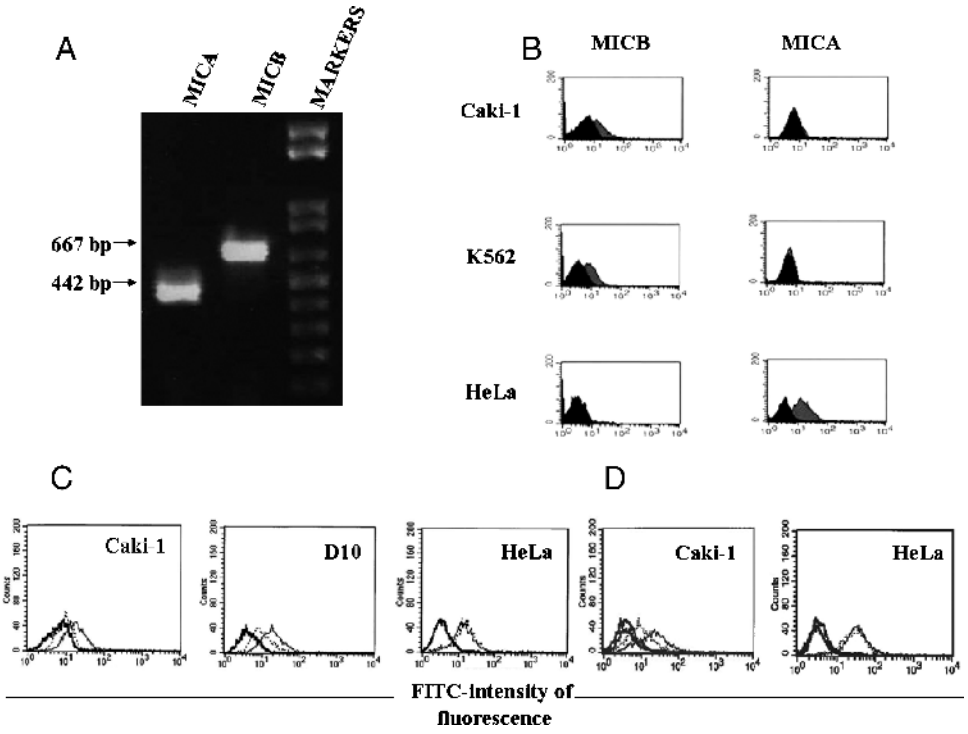

Figure 3. MICA and MICB gene and protein expressions in Caki-1 cells. (A) *MICA* (442 bp) and *MICB* (677 bp) transcripts were amplified by polymerase chain reaction from Caki-1 cDNA by using a single *MICA/B* sense primer and two *MICA*- or *MICB*-specific antisense primers as indicated in the Materials and Methods section. (B) The indicated tumor cell lines were stained either with a commercial APC-conjugated anti-MICB (left panel, gray areas) or with a commercial PE-conjugated anti-MICA (right panel, gray areas). The black areas show the intensity of fluorescence upon staining with APC- or PE-conjugated matching isotype mAbs. (C) The indicated tumor cell lines (1×10^6) were permeabilized and incubated with WW6B7 mAb (solid lines) or WW2G8 mAb (dashed lines) or an isotype-matched IgG1 mAbs (solid thick lines). After a 30-minute incubation in ice, cells were washed, and FITC-conjugated goat anti–mouse $F(ab)_2$ were added to the cell pellet. Cells were then analyzed by flow cytometry. (D) Nonpermeabilized (dashed lines) or permeabilized (solid lines) cells (1×10^6) were incubated with WW6B7 mAb and stained with a FITC-conjugated goat anti–mouse $F(ab)_2$ antibodies. The overlapping solid thick lines show the fluorescence given by control isotype IgG1 mAbs in nonpermeabilized or in permeabilized tumor cells.

cells, resting or IL-2–activated PBMCs were cultured in the presence or absence of Caki-1 cells. After 8 hours of incubation at 37°C, percentages of apoptotic and/or necrotic $CD56^+$ cells were evaluated by flow cytometry using annexin V and propidium iodide staining, respectively. To control the effect of the cell density on $CD56^+$ cells, the total number of $CD56^+$ cells cultured in the absence of Caki-1 cells was equal to that of the mix of $CD56^+$ and Caki-1 cells cultured in each experiment. Data from a representative experiment shown in Figure 4*A* indicated that unstimulated $CD56^+$ cells included approximately 7.5% of apoptotic cells and 27% of cells in transition from apoptosis to necrosis. In contrast, in the presence of Caki-1 cells, the percentage of apoptotic $CD56^+$ cells rose up to 16%, whereas that of the cells in transition rose up to 57%. In the presence of IL-2 and in the absence of Caki-1 cells, the percentage of damaged $CD56^+$ cells was reduced to 9.4%, whereas percentages of apoptotic or apoptotic/necrotic cells in the presence of Caki-1 RCC cells were similar (22% and 41%, respectively) to those observed in resting $CD56^+$ cells. To evaluate the specificity of Caki-1–induced NK cell apoptosis, we separately cultured–IL-2 activated PBMCs obtained from $HLA\text{-}A0201^+$ donors with IL-2–stimulated PBMCs obtained from three distinct $HLA\text{-}A0201^-$ healthy donors, Caki-1 cells, and HCT116 CRC cell line. To prevent IL-2–stimulated NK cell killing machinery upon conjugation with IL-2–stimulated allogeneic PBMCs, cells were cultured in CM supplemented with a high-dose concentration of concanamycin A (0.3 μM). Figure 5 shows that Caki-1 and HCT116 clearly induced NK cell apoptosis, whereas IL-2–activated HLA-A0201-negative PBMCs did not, suggesting that NK cells were preferentially affected by RCC and CRC cell lines in the presence of an inhibitor of NK cell killing machinery.

RCC Caki-1 Cells Preferentially Eliminate $CD56^+CD16^+$ Cell Subset

We then asked which NK cell subset is affected by the interaction with RCC Caki-1 cells. Peripheral blood mononuclear cells were cultured for 3 to 4 days at 37°C in CM in the presence of IL-2. Cells were then incubated overnight in the presence or absence of Caki-1 cells. Nonadherent cells were harvested and stained with a FITC-conjugated anti-CD16 or a PE-conjugated anti-CD56 mAb. Table 2 shows that, in the presence of Caki-1 cells, percentages of $CD56^+$ $CD16^+$ cells but not $CD56^+CD16^-$ cells in PBMC from five of

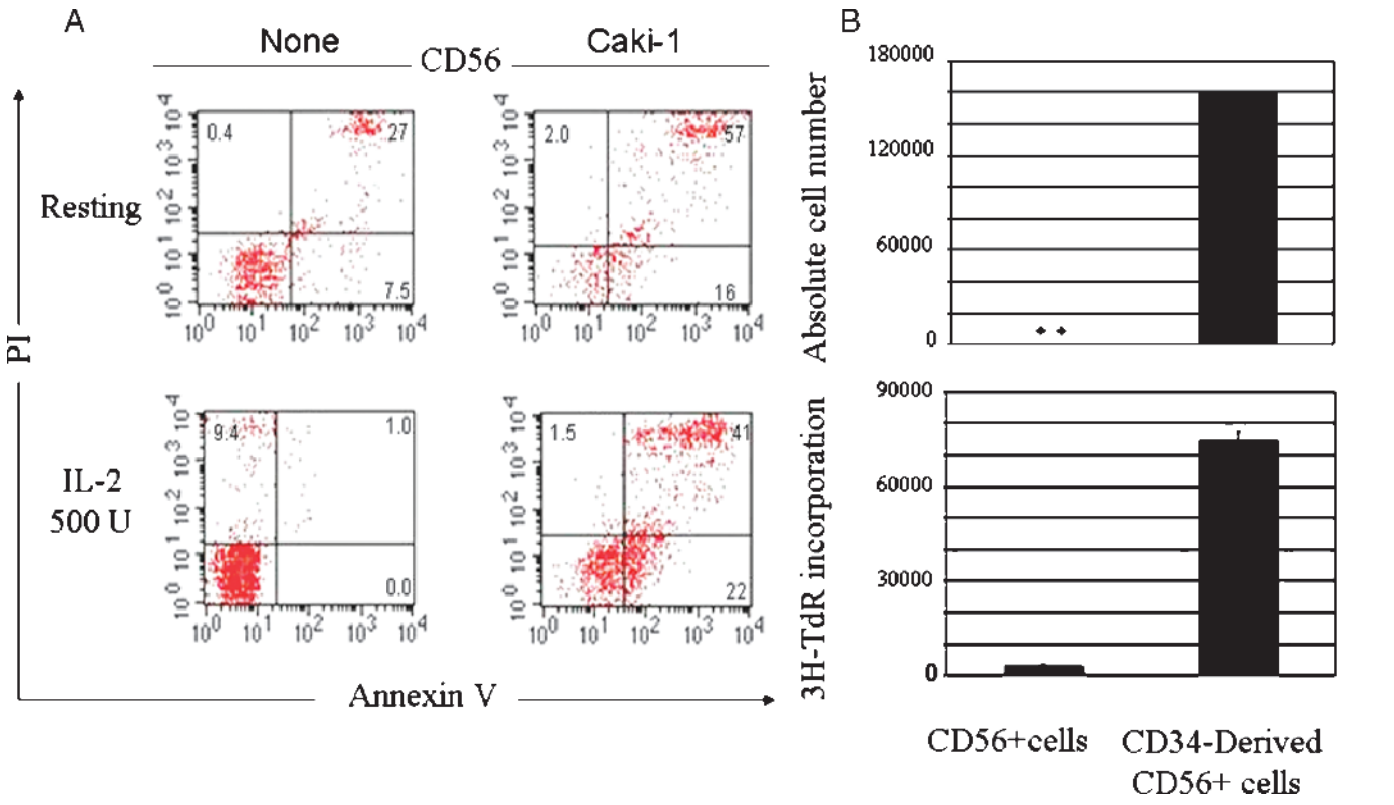

Figure 4. Caki-1 cells induce $CD56^+$ cells elimination upon effectors/target cell interaction. (A) Peripheral blood mononuclear cells were cultured in the presence or absence of 500 U of IL-2. After a 4-day culture at 37°C, cells were harvested and subjected to a Ficoll/Hypaque gradient separation. Cells were then cultured in the presence or absence of Caki-1 cells at a 5:1 effector/target ratio at 37°C in a 5% CO_2 incubator. After 8 hours, nonadherent cells were harvested and stained as indicated in the Materials and Methods section. Peripheral blood mononuclear cells were analyzed by flow cytometry as indicated by defining an electronic gate on $CD56^+$ cells. This figure shows one of three experiments performed with similar results. (B) Peripheral blood mononuclear cells were cultured for 4 days in the presence of IL-2 (500 U/ml), whereas immature $CD56^+$ cells were obtained from G-CSF–mobilized PB $CD34^+$ cells cultured in the presence of IL-2 and SCF for 21 days. Peripheral blood–$CD56^+$ cells and immature $CD56^+$ cells were magnetically sorted and cultured (1.5×10^5) in the presence of K562 cells at a 2:1 effector/target ratio. After a 3-day culture, $CD56^+$ cells were magnetically sorted and counted (upper panel). Subsequently, aliquots of the same cell cultures depleted of $CD56^+$ cells were transferred in a 96-U/well and left to proliferate for 2 days. Proliferation was then measured by ^{3}H-thymidine incorporation (lower panel). This figure shows one of three experiments performed with similar results.

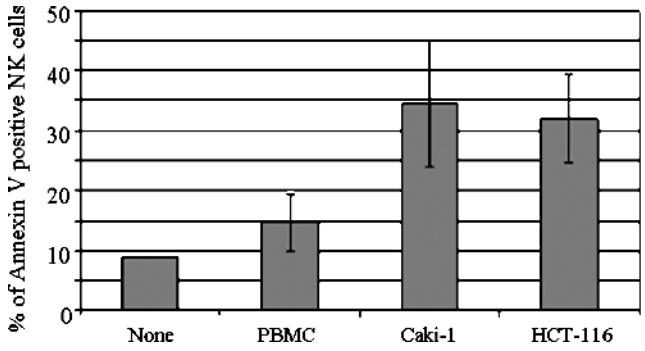

Figure 5. Natural killer cell apoptosis is preferentially induced by cancer cells. Peripheral blood mononuclear cells of an HLA-A0201$^+$ healthy donor and PBMCs of three HLA-A0201$^-$ healthy donors were cultured in the presence of IL-2 (200 U/ml) for 5 days. HLA-A0201$^+$ PBMCs were then harvested and cultured in the absence or presence of IL-2–stimulated HLA-A0201$^-$ PBMCs from donors 1, 2, and 3, respectively. Caki-1 and HCT116 cells were used as positive controls. This figure shows cumulative data regarding the effects of PBMCs of the indicated HLA-A0201$^-$ donors on HLA-A0201$^+$ NK cells, whereas Caki-1 and HCT116 representing the effects of Caki-1 and HCT116 on HLA-A0201–positive and –negative cells are also reported. All of the cell culture conditions which included NK cells in the absence or presence of allogeneic PBMC or in the presence of cancer cell lines were supplemented with concanamycin A (0.3 μM).

six healthy individuals were significantly reduced compared with PBMCs cultured in the absence of Caki-1 cells (P = .02), suggesting that Caki-1 cells eliminated cytotoxic NK cells without affecting regulatory CD56$^+$CD16$^-$ NK cells.

Preferential Elimination of Terminally Differentiated NK Cells upon Interaction with Target Cells

Similar results were obtained when we cultured magnetically sorted PB CD56$^+$ cells with the NK cell–sensitive cell line, K562. After a 3-day culture at 37°C, viable PB-CD56$^+$ cells were separated from K562 cells by magnetic sorting. Figure 4*B* shows that noncytotoxic, immature, CD56$^+$CD16$^-$ cells (generated from granulocyte colony-stimulating factor mobilized CD34$^+$ cells) [14] were clearly recovered, whereas PB-derived CD56$^+$ cells were not (Figure 4*B*, *upper panel*) suggesting that IL-2–activated PB-CD56$^+$ cells were eliminated upon interaction with target cells. To determine whether sorted PB-CD56$^+$ and immature NK cells affected K562 proliferation, aliquots of K562 cell cultures depleted of PB-CD56$^+$ or immature NK cells (shown in Figure 4*B*, *lower panel*) were further cultured as indicated in the Materials and Methods section. After a 3-day incubation, we observed K562 cell proliferation after culture in the presence of immature NK cells. In contrast, there was no K562 proliferation after culture in the presence of PB-CD56$^+$ cells (Figure 4*B*, *lower panel*).

Caki-1–Dependent NK Cell Apoptosis Involves CD18

Caki-1 cell–dependent NK cell elimination did not require NKG2D blockade and granule exocytosis because addition of a blocking anti-NKG2D mAb or concanamycin A did not improve NK cell recovery (data not shown). Furthermore, Table 3 shows that the elimination of NK cells by FAS ligand–negative Caki-1 cells (data not shown) was also unaffected by the addition of optimal concentrations of the general caspase inhibitor, Z-VAD-FMK, to the cultures, suggesting that the NK cell elimination by Caki-1 cells was caspase- and FAS-independent. Using an anti-CD18 mAb, however, Caki-1–dependent NK cell apoptosis was significantly reduced. In contrast, as expected, CD56$^+$CD16$^-$ cells were 8.1 ± 3.3% of the total NK cells and they were not negatively affected neither by Caki-1 cells (27 ± 8.4%) nor by HCT116 cells (16.3 ± 0.4%). Figure 6, *upper panel*, shows a dose-response experiment showing the effect of such mAb on CD56$^+$CD16$^+$ cells of healthy donors after 12 hours of incubation with intercellular adhesion molecule 1 (ICAM-1$^+$) Caki-1 cells. To further investigate whether this observation was restricted to Caki-1 cells, we included in the outlined experiment a MICA/B$^+$, ICAM-1$^-$ CRC cell line, HCT116. Conversely, Figure 6, *lower panel*, shows that HCT116 cells triggered NK cell apoptosis, which was significantly reduced when NK cells and HCT116 were cultured in the presence of logarithmic concentration doses of anti-CD18, suggesting that Caki-1– and HCT116-dependent NK cell apoptosis may depend on NK–cancer cell conjugation that could at least involve CD18 on NK cells and ICAM-1 on cancer cells. Notably, NK cell apoptosis inhibition was never complete, suggesting that molecules other than CD18 may also be involved.

Discussion

Renal cell carcinoma is considered an immunogenic tumor because spontaneous regressions and long-lasting complete remissions in a small subset of patients undergoing adoptive lymphokine-activated killer cell

Table 2. Caki-1 Cells Induce Elimination of CD56$^+$CD16$^+$ Cell Subset without Affecting CD56$^+$ CD16$^-$ NK Cells*.

	Caki-1 Cells			
	–	–	+	+
	CD56$^+$CD16$^+$ (%)	CD56$^+$CD16$^-$ (%)	CD56$^+$CD16$^+$ (%)	CD56$^+$CD16$^-$ (%)
Case				
1	14	9.4	5.83	12.6
2	7.9	7.6	7.6	8.4
3	12.5	10.8	0.9	7.7
4	9.4	8.5	2.3	10.2
5	4.8	8.4	0.9	10
6	1.4	7.9	0.0	2.8
Mean ± SD	8.3 ± 4.7	8.7 ± 1.1	**2.8 ± 2.8**†	8.6 ± 3.3

*Peripheral blood mononuclear cells were cultured in the presence of IL-2 as detailed in the Materials and Methods section before culture in the presence or absence of Caki-1 RCC cells.
† t test: CD16$^+$ *versus* CD16$^+$/Caki-1, P = .02; CD16$^+$/Caki-1 *versus* CD16$^-$/Caki-1, P = .007; bolded numbers, statistically significant differences.

Table 3. Caki-1 Cells Induced Elimination of CD56$^+$CD16$^+$ Cell Subset Is Caspase-Independent*.

Experiments	Caki-1 Cells			
	–	–	+	+
	–	Z-VAD (40 μM)	–	Z-VAD (40 μM)
1	12.5	8.0	0.91	1.08
2	5.0	3.91	0.95	0.93
3	9.4	9.28	2.32	3.05
Mean ± SD†	8.96 ± 3.7	7.0 ± 2.8	1.39 ± 0.8	1.68 ± 1.1

*Peripheral blood mononuclear cells were cultured in the presence of IL-2 with or without Z-VAD-FMK as detailed in the Materials and Methods section before culture in the presence or absence of Caki-1 RCC cells.
† t test: CD56$^+$CD16$^+$ cells *versus* CD56$^+$CD16$^+$ cells + Z-VAD-FMK, P = .52; CD56$^+$CD16$^+$ cells + Caki-1 cells *versus* CD56$^+$CD16$^+$ cells + Caki-1 cells + Z-VAD-FMK, P = .740; CD56$^+$CD16$^+$ cells *versus* CD56$^+$CD16$^+$ cells + Caki-1 cells, P = .02; CD56$^+$CD16$^+$ cells *versus* CD56$^+$CD16$^+$ cells *versus* CD56$^+$CD16$^+$ cells + Caki-1 cells + Z-VAD-FMK, P = .03.

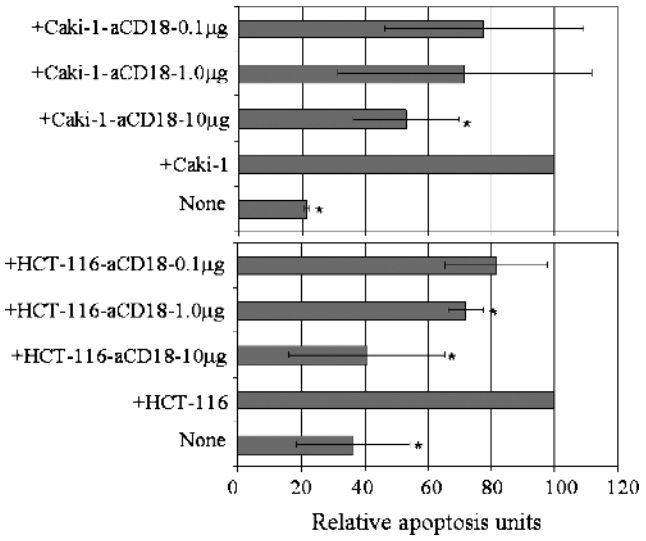

Figure 6. Natural killer cell apoptosis upon NK/cancer cell interaction involves CD18. After 4 days of incubation with IL-2, PBMCs were cultured in the presence of Caki-1 cells (upper panel) or HCT116 (lower panel) with or without logarithmic concentration doses (μg/ml) of an anti-CD18 mAb at 4:1 ratio, respectively. After 12 hours of culture, nonadherent cells were harvested and stained as indicated in the Materials and Methods section. Apoptotic $CD56^+CD16^+$ cells were identified as $CD56^+CD16^+$annexin V^+ cells by analyzing the percentage of green fluorescent cells falling within an electronic gate surrounding $CD56^+CD16^+$ cells. This figure summarizes the results obtained from three different donors. Asterisks indicated statistically significant differences ($P \leq .05$).

cell and/or IL-2 immunotherapy have been observed [3]. Why such response occurs is unknown. Signs of local immune activation have been described including the presence of cellular infiltrates composed of $CD4^+$ and $CD8^+$ T cells and dendritic cells [8]. Interestingly, after enzymatic digestion of RCC lesions, Schleypen et al. [6] have isolated two populations of NK cells. One was $CD56^{bright}$ $CD16^{negative}$ and did not lyse K562 cells, whereas the other one was $CD56^{low}$ $CD16^{positive}$ and acquired an efficient cytotoxic activity to K562 cells upon IL-2 activation. The ineffectiveness of the first NK cell subset may be due to its harboring a population of myeloid cells because a subset of CD56-positive monocyte/macrophage with antiproliferative activity on tumor cell lines [14,16,17] has been described recently.

Natural killer cell cytotoxicity is regulated by a balanced activation of KIRs and natural cytotoxic receptors. Killer inhibitory receptors bind HLA-class I molecules delivering an inhibitory signal upon recruitment of tyrosine phosphates [18]. NKG2D is a major NK cell–activating receptor that binds stress-induced nonclassic HLA-class I molecules MICA, MICB, and UL16-binding proteins [19,20].

According to the missing self hypothesis, host NK cells may kill autologous cancer cells only when malignant cells do not express HLA-class I antigens. Although loss of HLA-class I expression has been described in a variety of solid tumors [21], myeloid leukemia cells express high levels of HLA-class I antigens. However, they can still be killed by HLA-matched class I NK cells, suggesting that HLA-class I expression *per se* is not sufficient to prevent NK cell cytotoxicity [11].

Currently, there are enough data suggesting that *de novo* expression of NKG2DL on HLA-matched cancer cells overrides the inhibitory activity of KIRs leading to cancer cell elimination [11,22,23].

The relationship occurring among NK cells, RCC cells, and RCC tumor microenvironment is poorly characterized. Taking advantage of the availability of a RCC TMA, we assessed NKG2DL expression in RCC lesions obtained from 140 patients with RCC. We clearly demonstrated that RCC cells expressed high levels of cytoplasmic and cell surface MICA/B in more than 95% of the TMA punches analyzed. Notably, we could not find any correlation between the expression of MICA/B and RCC clinical stages. To address mechanisms underlying defective NK cell infiltration of RCC, we evaluated the distribution of MICA and MICB in RCC cells analyzing their gene and protein expressions.

The finding that despite *MICA* gene expression, only a low level of MICB antigen is correctly expressed on RCC cell, is intriguing. Our data suggest that MICA is transcribed but not translated, whereas a fraction of MICB may be retained into the cytoplasm of Caki-1 cells. As a result, there may be a suboptimal level of expression of NKG2DLs on the cell surface of RCC cells.

Although we were not able to determine whether RCC lesions expressed MICA or MICB, it is likely to hypothesize that they express MICB because 1) we could detect MICB in RCC Caki-1 cells both intracellularly and on cell surfaces, but we could not detect MICA protein, despite *MICA* gene expression; 2) the location of MICA/B in TMA cancer cells resembled that observed in Caki-1 cells; and 3) according to Groh et al. [24], two of two RCC lesions were stained by a MICA/B–specific mAb, but none of them was stained by a MICA-specific mAb. Clearly, this conclusion will be strengthened by results obtained by staining RCC TMA with an MICB-specific mAb.

The expression of MICA/B in most RCC cells might expose them to NK cell recognition through NKG2D. Therefore, we investigated infiltration by NK cells in the tumor milieu. We considered NK as those cells coexpressing CD56 and CD16 markers. Surprisingly, we found very low levels of NK cell infiltration in RCC, whereas inflammatory interstitial cells were mainly $CD16^+CD56^-$.

Morphologic and phenotypic analysis of $CD16^+CD56^-$ cells has demonstrated that these cells resemble monocyte/macrophage cell types. This observation was confirmed by the expression of CD68 in the TMA specimens.

$CD16^+CD68^+CD56^-$ myeloid cells are a small subset representing less than 10% of PB monocytes [25,26]. They expand in different conditions including sepsis and human immunodeficiency virus infection [27,28]. Interestingly, $CD16^+$ PB monocytes promptly expand in a variety of malignancies to become approximately 40% of the total monocyte population. Furthermore, such expansion becomes even higher, reaching 80% of the total population, when patients are treated with recombinant human macrophage colony-stimulating factor [29]. In the early 1990s, van Ravenswaay Claasen et al. [30] showed that there was an infiltration of $CD16^+$ macrophages in RCC, melanoma, and CRC lesions, and they hypothesized a role of these cells in antitumor cytotoxicity. We also identified a strong $CD16^+$ macrophage infiltration in most of our clinically and pathologically well-documented collection of 140 RCC lesions. However, importantly, our statistical analysis has shown that $CD16^+$ macrophage infiltration is associated with RCC metastasis. In addition, there was a trend toward an association with poorly differentiated RCC cells.

The role of $CD16^+$ macrophages in RCC milieu is unclear. $CD16^+$ monocytes are reported to be functionally different from the predominant population of $CD14^+$ monocytes. Consistent with their ability to be strong producers of tumor necrosis factor α [31], minimal

producers of IL-10 [26,31], and proliferative inhibitors [16,17], they are considered powerful inflammatory cells. It is possible that $CD16^+$ monocytes play a role in regulating tumor immunosurveillance because their frequency is strongly increased at a systemic level in a variety of advanced malignancies [29,32,33]. To date, the reasons why $CD16^+$ monocytes specifically expand in the PB of patients with malignancies are unknown. One possibility is that advanced solid tumors may release factors causing $CD16^+$ monocyte expansion [29] or chemoattracting them on tumor sites [34,35].

Conversely, our *in vitro* data strongly suggest that $CD16^+$ NK cells undergo apoptosis upon interaction with target cells, including RCC, Caki-1, myeloid leukemia, K562 and CRC, HCT116-derived cell lines, thereby providing a mechanistic explanation to the relative absence of these lymphocytes from the RCC microenvironment.

We attempted to explore molecular mechanisms by which cancer cell lines induced RCC apoptosis. We hypothesized an involvement of a caspase-dependent mechanism or/and a granule exocytosis-dependent mechanism eventually due to a "friendly fire" situation triggered by NK cell upon conjugation with cancer cells and after granule exocytosis. Therefore, we used Z-VAD, a potent general caspase inhibitor, and concanamycin A, a specific inhibitor of a granule-dependent cytotoxicity. Both inhibitors failed to prevent NK cell elimination by Caki-1, FAS ligand–negative and HCT116, FAS ligand–positive cells suggesting that this phenomenon is caspase-, perforin-, and FAS-independent and also excluding that the possibility of perforin spilling in the intercellular area of effector/target cell surface may cause autologous NK damage.

Natural killer cells could be also damaged directly and/or indirectly by myeloid cells resident in the tumor microenvironment. Resident myeloid cells could impair the function of the host's NK cells through an alteration of the metabolism of L-tryptophan, L-arginine, and arachidonic acid and by producing nitric oxide [36,37]. In our experience, the Caki-1–dependent elimination of NK cells was not affected by the depletion of monocytes from cell cultures used for *in vitro* experiments (Sconocchia et al., unpublished data). Obviously, to make any clear conclusions, further studies are required.

CD18 is a cell surface receptor composed of a constant chain that is associated with a distinct α chain to characterize four distinct cell surface molecules including CD11a (LFA-1), CD11b (MAC-1), CD11c, and CD11d. CD18 is expressed on NK cells mainly as LFA-1 and MAC-1. CD18 is also involved in NK cytotoxicity and cell adhesion because LFA-1 contributes to NK cytotoxicity. Anti-CD18 was able to reduce partially the annexin V expression on cytotoxic NK cells upon conjugation with cancer cells. Thus, it is possible to assume that, in normal conditions, different levels of β_2-integrin ligands on the cell surface of cancer cells may regulate the extent of NK cell apoptosis.

Recently, it has been shown that neutrophil β_2-integrins regulate neutrophil apoptosis through the activation of nuclear factor κ light chain enhancer of activated B cells and mitogen-activated protein kinase–extracellular signal–regulated kinase [38]. Thus, we hypothesize that CD18 ligation of LFA-1 and MAC-1 on NK cells could affect NK cells' survival upon cancer cell interaction. Our data suggest that the disruption of the interaction between CD18 on NK cells and ICAM-1 on Caki-1 cells partially prevents Caki-1 cell–dependent apoptosis. In contrast, it is not clear how NK cell's CD18 is affecting HCT116-dependent NK cell apoptosis because our HCT116 cells are ICAM-1–negative. One possible explanation could reside on the fact that CD18 interacts with different CD18 ligands including ICAM-2, ICAM-3, and ICAM-4, which could be expressed on HCT116, CRC cells.

Finally, our data suggest that other than CD18, additional molecules could be involved in regulating NK cell survival upon conjugation with target cells including CD16. Infect, ligation of CD16 on NK cells caused loss of cell surface CD16 expression [39]. However, it is not completely understood whether the effect is a result of CD16 internalization or NK cells' elimination.

The identification of strategies possibly improving cytostatic and antigen-presenting functions of $CD16^+$ myeloid cells and delaying NK cell apoptosis in the presence of cancer cells may help restore an efficient immune response in RCC patients.

Acknowledgments

The authors thank Mirko Vukcevic for providing PBMC and Goffredo Davoli for manuscript revision. The authors declare no conflict of interest.

References

[1] Motzer RJ, Bander NH, and Nanus DM (1996). Renal-cell carcinoma. *N Engl J Med* **335**, 865–875.

[2] Motzer RJ and Russo P (2000). Systemic therapy for renal cell carcinoma. *J Urol* **163**, 408–417.

[3] Thompson JA, Shulman KL, Benyunes MC, Lindgren CG, Collins C, Lange PH, Bush WH Jr, Benz LA, and Fefer A (1992). Prolonged continuous intravenous infusion interleukin-2 and lymphokine-activated killer-cell therapy for metastatic renal cell carcinoma. *J Clin Oncol* **10**, 960–968.

[4] Tomita Y, Katagiri A, Saito K, Imai T, Saito T, Tanikawa T, Terunuma M, Nishiyama T, and Takahashi K (1998). Adoptive immunotherapy of patients with metastatic renal cell cancer using lymphokine-activated killer cells, interleukin-2 and cyclophosphamide: long-term results. *Int J Urol* **5**, 16–21.

[5] Childs R, Chernoff A, Contentin N, Bahceci E, Schrump D, Leitman S, Read EJ, Tisdale J, Dunbar C, Linean WM, et al. (2000). Regression of metastatic renal-cell carcinoma after nonmyeloablative allogeneic peripheral-blood stem-cell transplantation. *N Engl J Med* **343**, 750–758.

[6] Schleypen JS, Baur N, Kammerer R, Nelson PJ, Rohrmann K, Grone EF, Hohenfellner M, Haferkamp A, Pohla H, Schendel DJ, et al. (2006). Cytotoxic markers and frequency predict functional capacity of natural killer cells infiltrating renal cell carcinoma. *Clin Cancer Res* **12**, 718–725.

[7] Seliger B, Atkins D, Bock M, Ritz U, Ferrone S, Huber C, and Storkel S (2003). Characterization of human lymphocyte antigen class I antigen-processing machinery defects in renal cell carcinoma lesions with special emphasis on transporter-associated with antigen-processing down-regulation. *Clin Cancer Res* **9**, 1721–1727.

[8] Frankenberger B, Noessner E, and Schendel DJ (2007). Immune suppression in renal cell carcinoma. *Semin Cancer Biol* **17**, 330–343.

[9] Moretta A, Biassoni R, Bottino C, Mingari MC, and Moretta L (2000). Natural cytotoxicity receptors that trigger human NK-cell–mediated cytolysis. *Immunol Today* **21**, 228–234.

[10] Kampbell KS and Colonna M (2001). Human natural killer cell receptors and signal transduction. *Int Rev Immunol* **20**, 333–370.

[11] Sconocchia G, Lau M, Provenzano M, Rezvani K, Wongsena W, Fujiwara H, Hensel N, Melenhorst J, Li J, Ferrone S, et al. (2005). The antileukemia effect of HLA-matched NK and NK–T cells in chronic myelogenous leukemia involves NKD2D–target-cell interactions. *Blood* **106**, 3666–3672.

[12] Cerwenka A, Baron JL, and Lanier LL (2001). Ectotopic expression of retinoic acid early inducible-1 gene (RAE-1) permits natural killer cell–mediated rejection of a MHC class I–bearing tumor *in vivo*. *Proc Natl Acad Sci USA* **98**, 11521–11526.

[13] Kohler G and Milstein C (1975). Continuous cultures of fused cells secreting antibody of predefined specificity. *Nature* **256**, 495–497.

[14] Sconocchia G, Fujiwara H, Rezvani K, Keyvanfar K, El Ouriaghli F, Grube M, Melenhorst J, Hensel N, and Barret AJ (2004). G-CSF–mobilized $CD34^+$ cells cultured in interleukin-2 and stem cell factor generate a phenotypically novel monocyte. *J Leukoc Biol* **76**, 1214–1219.

[15] Jinushi M, Takehara T, Tatsumi T, Kanto T, Groh V, Spies T, Kimura R, Miyagi T, Mochizuki K, Sasaki Y, et al. (2003). Expression and role of MICA and MICB in human hepatocellular carcinomas and their regulation by retinoic acid. *Int J Cancer* **104**, 354–361.

[16] Sconocchia G, Del Principe D, and Barret AJ (2007). CD16 (low/negative) tumor-infiltrating lymphocyte: lymphoid or myeloid in origin? *Clin Cancer Res* **13**, 1620.

[17] Sconocchia G, Keyvanfar K, El Ouriaghli F, Grube M, Rezvani K, Fujiwara H, McCoy JP Jr, Hensel N, and Barret AJ (2005). Phenotype and function of a $CD56^+$ peripheral blood monocyte. *Leukemia* **19**, 69–76.

[18] Bruhns P, Marchetti P, Fridman WH, Vivier E, and Daeron M (1999). Differential roles of N- and C-terminal immunoreceptor tyrosine–based inhibition motifs during inhibition of cell activation by killer cell inhibitory receptors. *J Immunol* **162**, 3168–3175.

[19] Bauer S, Groh V, Wu J, Steinle A, Phillips JH, Lanier LL, and Spies T (1999). Activation of NK cells and T cells by NKG2D, a receptor for stress-inducible MICA. *Science* **285**, 727–729.

[20] Sutherland CL, Chalupny NJ, and Cosman D (2001). The UL16-binding proteins, a novel family of MHC class I–related ligands for NKG2D, activate natural killer cell functions. *Immunol Rev* **181**, 185–192.

[21] Chang CC, Campoli M, and Ferrone S (2004). HLA class I antigen expression in malignant cells: why does it not always correlate with CTL-mediated lysis? *Curr Opin Immunol* **16**, 644–650.

[22] Doubrovina ES, Doubrovin MN, Vider E, Sisson RB, O'Reilly RJ, Dupont B, and Vyas YM (2003). Evasion from NK cell immunity by MHC class I chain–related molecules expressing colon adenocarcinoma. *J Immunol* **171**, 6891–6899.

[23] Carbone E, Neri P, Mesuraca M, Fulciniti MT, Otsuki T, Pende D, Groh V, Spies T, Pollio G, Cosman D, et al. (2005). HLA class I, NKG2D, and natural cytotoxicity receptors regulate multiple myeloma cell recognition by natural killer cells. *Blood* **105**, 251–258.

[24] Groh V, Rhinehart R, Secrist H, Bauer S, Grabstein KH, and Spies T (1999). Broad tumor-associated expression and recognition by tumor-derived gamma delta T cells of MICA and MICB. *Proc Natl Acad Sci USA* **96**, 6879–6884.

[25] Ziegler-Heitbrock HW, Passlick B, and Flieger D (1988). The monoclonal antimonocyte antibody My4 stains B lymphocytes and two distinct monocyte subsets in human peripheral blood. *Hybridoma* **7**, 521–527.

[26] Ziegler-Heitbrock HW (1996). Heterogeneity of human blood monocytes: the $CD14^+CD16^+$ subpopulation. *Immunol Today* **17**, 424–428.

[27] Thieblemont N, Weiss L, Sadeghi HM, Estcourt C, and Haeffner-Cavaillon N (1995). $CD14^{low}CD16^{high}$: a cytokine-producing monocyte subset which expands during human immunodeficiency virus infection. *Eur J Immunol* **25**, 3418–3424.

[28] Fingerle G, Pforte A, Passlick B, Blumenstein M, Strobel M, and Ziegler-Heitbrock HW (1993). The novel subset of $CD14^+/CD16^+$ blood monocytes is expanded in sepsis patients. *Blood* **82**, 3170–3176.

[29] Saleh MN, Goldman SJ, Lo Buglio AF, Beall AC, Sabio H, McCord MC, Minasian L, Alpaugh RK, Weiner LM, and Munn DH (1995). $CD16^+$ monocytes in patients with cancer: spontaneous elevation and pharmacologic induction by recombinant human macrophage colony-stimulating factor. *Blood* **85**, 2910–2917.

[30] van Ravenswaay Claasen HH, Kluin PM, and Fleuren GJ (1992). Tumor infiltrating cells in human cancer. On the possible role of $CD16^+$ macrophages in antitumor cytotoxicity. *Lab Invest* **67**, 166–174.

[31] Belge KU, Dayyani F, Horelt A, Siedlar M, Frankenberger M, Frankenberger B, Espevick T, and Ziegler-Heitbrock L (2002). The proinflammatory $CD14^+CD16^+$ DR^{++} monocytes are a major source of TNF. *J Immunol* **168**, 3536–3542.

[32] Dayyani F, Joening A, Ziegler-Heitbrock L, Schmidmaier R, Straka C, Emmerich B, and Meinhardt G (2004). Autologous stem-cell transplantation restores the functional properties of $CD14^+$ $CD16^+$ monocytes in patients with myeloma and lymphoma. *J Leukoc Biol* **75**, 207–213.

[33] Melichar B, Touskova M, and Vesely P (2002). Effect of irinotecan on the phenotype of peripheral blood leukocyte populations in patients with matastatic colorectal cancer. *Hepatogastroenterology* **49**, 967–970.

[34] Allavena P, Sica A, Solinas G, Porta C, and Mantovani A (2008). The inflammatory micro-environment in tumor progression: the role of tumor-associated macrophages. *Crit Rev Oncol Hematol* **66**, 1–9.

[35] Mantovani A, Romero P, Palucka AK, and Marincola FM (2008). Tumor immunity: effector response to tumor and role of the microenvironment. *Lancet* **371**, 771–783.

[36] Gallina G, Dolcetti L, Serafini P, De Santo C, Marigo I, Colombo MP, Basso G, Brombacher F, Borrello I, Zanovello P, et al. (2006). Tumors induce a subset of inflammatory monocytes with immunosuppressive activity on $CD8^+$ cells. *J Clin Invest* **116**, 2777–2790.

[37] Viola A and Bronte V (2007). Metabolic mechanisms of cancer-induced inhibition of immune responses. *Semin Cancer Biol* **17**, 309–316.

[38] Mayadas TN and Cullere X (2005). Neutrophil β_2 integrins: moderators of life or death decisions. *Trends Immunol* **26**, 388–395.

[39] Jewett A, Cacalano NA, Head C, and Teruel A (2006). Coengagement of CD16 and CD94 receptors mediates secretion of chemokines and induces apoptotic death of naive natural killer cells. *Clin Cancer Res* **12**, 1994–2003.